

1 *Renewable Energy*

2 *Volume 48, December 2012, Pages 251–262*

3 **Reliability Analysis for Hydrokinetic Turbine Blades**

4  
5  
6  
7 **Zhen Hu and Xiaoping Du\***

8  
9 Department of Mechanical and Aerospace Engineering  
10 Missouri University of Science and Technology  
11 Rolla, Missouri 65409, U.S.A.  
12  
13  
14  
15

16 **\*Corresponding author**

17 Dr. Xiaoping Du

18 Associate Professor of Mechanical Engineering  
19 Department of Mechanical and Aerospace Engineering  
20 Missouri University of Science and Technology  
21 400 West 13th Street, Toomey Hall 290D,  
22 Rolla, MO 65401, U.S.A.  
23 Tel: 1-573-341-7249  
24 Fax: 1-573-341-4607  
25 E-mail: [dux@mst.edu](mailto:dux@mst.edu)  
26

## **Abstract**

Reliability is an important element in the performance of hydrokinetic turbines. It is also a driving factor of the system lifetime cost. In this paper, we perform time-dependent reliability analysis for the blades of a river-based horizontal-axis hydrokinetic turbine. Based on the stochastic representation of the monthly river velocity and material strength, a limit-state function is established with the classical blade element momentum method. In the limit-state function, a failure is defined as the event when the flapwise bending moment exceeds the allowable moment that corresponds to the ultimate strength of the material. The upcrossing rate method is employed to calculate the time-dependent reliability of the hydrokinetic turbine blade over its design life period. The results indicate that setting a proper cut-out river velocity is important for the reliability of the hydrokinetic turbine blade.

**Keywords:** Reliability, hydrokinetic turbine, time-dependent, cut-out velocity

1 **1. Introduction**

2 Hydrokinetic energy refers to energy generated from the ocean wave, current, tidal, and in-  
3 stream current energy resources. It has received increasing attention recently [1-7] because it can  
4 provide supplies of clean, renewable energy for the world's carbon-free energy demand [3, 5].  
5 Several technologies have been developed to extract hydrokinetic energy, such as float or buoy  
6 systems and oscillating water column devices. Among these technologies, hydrokinetic turbines  
7 are one of the most commonly used, especially in inland rivers. The hydrokinetic turbine  
8 technology is still under development and has not been fully commercialized yet. One factor,  
9 which plays a vital role in the commercialization, is the reliability of hydrokinetic turbines. The  
10 reliability is directly associated with the availability of the hydrokinetic turbine and its energy-  
11 cost ratio. It is one of the core elements to be considered during the development phase of the  
12 hydrokinetic turbine.

13 The Failure Modes and Effect Analysis (FMEA) of wind turbines has shown that the turbine  
14 blades have the highest risk priority number [8-9], and the safety of the turbine blade should be  
15 given a special consideration during the design of the wind turbine. We expect that it is the same  
16 case for a hydrokinetic turbine because it shares similarities with a wind turbine. In addition, for  
17 a hydrokinetic turbine, there are uncertainties inherent in the river environment, the stress of the  
18 turbine blades, and the resistance of materials. Their impact on the reliability of blades should be  
19 evaluated during the blade design.

20 The technology of the hydrokinetic turbine is still under development, and the research on the  
21 reliability of hydrokinetic turbines has rarely been reported. But there are similarities between  
22 hydrokinetic turbines and wind turbines. Because the technology of wind turbines is relatively  
23 mature, we can therefore use the results of the reliability analysis of wind turbines as a reference

1 for hydrokinetic turbines. The blades of both types of turbines have similar failure modes, such  
2 as fatigue and fracture due to ultimate loading. For hydrokinetic turbine blades, however, the  
3 natural climates, which govern the loading on the turbine blades, are different from those of wind  
4 turbine blades. One of the differences is that the river flow velocity has longer memory than the  
5 wind climate. In the past decades, several methods were developed to analyze the reliability of  
6 wind turbine blades. For example, Agarwal [10] proposed efficient extrapolation procedures to  
7 predict the long-term extreme loads for offshore wind turbines based on limited field data. By  
8 using inverse reliability, Saranyasontorn and Manuel [11-12] studied the reliability of wind  
9 turbines against extreme loads. Similarly, Ronold [13] proposed a nested reliability analysis  
10 method for analysis of the safety of a wind turbine rotor blade against failure in ultimate loading.  
11 However, these reliability analysis methods for wind turbine blades cannot be directly applied to  
12 the reliability of hydrokinetic turbine blades because as mentioned above, the wind environment  
13 is different from the river environment. Besides, most of the previous research has not  
14 considered the time influence on the loading of turbine blades.

15 The river loading varies over time, and there is some kind of seasonal characteristic in the  
16 monthly river velocity over a long time period. The monthly river velocity, which governs the  
17 loading of hydrokinetic turbine blades, is an auto-correlated stochastic process. The reliability of  
18 hydrokinetic turbine blades, therefore, also varies over time. Thus time-dependent reliability  
19 analysis is necessary for river-based hydrokinetic turbine blades.

20 The nested reliability method proposed by Ronold [13] can address the time-dependent  
21 problem by discretizing the time period into a series of time intervals. But it may not be feasible  
22 for the hydrokinetic turbine blade reliability analysis because the monthly river flow velocity has

1 much longer memory than the wind climates [14]. The Monte Carlo simulation (MCS) can be  
2 used, but it is computationally expensive.

3 For general time-dependent reliability analysis, many methods have been proposed in the past  
4 decades, including the Gamma distribution method and the Markov method. The most  
5 commonly used one is the upcrossing rate method [15-19]. This method is based on the Poisson  
6 assumption, and the key of this method is the calculation of the upcrossing rate. In order to  
7 increase the accuracy of computation, Sudret [20] proposed an analytical derivation of the  
8 upcrossing rate, and this method was used by Zhang and Du [21] later, for reliability analysis of  
9 function generator mechanisms over a certain time period. The upcrossing method can also be  
10 employed for the time-dependent reliability analysis of hydrokinetic turbine blades.

11 The purpose of this paper is to develop a time-dependent reliability analysis model for river  
12 based hydrokinetic turbine blades. We consider a horizontal-axis hydrokinetic turbine with three  
13 turbine blades. By accounting for the failure due to excessive flapwise bending moment, we  
14 compute the reliability of turbine blades over a 20-year design life. The stochastic characteristics  
15 of the monthly river velocity are modeled based on the monthly river discharge dataset of the  
16 Missouri river and the relationship between the river discharge and river velocity. The flapwise  
17 bending moment of the turbine blade is obtained using the classical blade element momentum  
18 model. And the upcrossing rate method is employed to carry out the reliability analysis.

19 In Section 2, we analyze the stochastic characteristics of the river flow velocity. Based on that,  
20 we establish a limit-state function using the blade element momentum theory. In Section 3, we  
21 explain the time-dependent reliability analysis method for hydrokinetic turbine blades, and an  
22 example is given in Section 4. Conclusions are provided in Section 5.

1 **2. Statement of problem**

2 In this section, we discuss the major factors that affect the reliability of the hydrokinetic  
3 turbine blades and then establish a limit-state function for the reliability analysis.

4

5 **2.1 River flow velocity**

6 *2.1.1 River flow velocity formulation*

7 The river flow velocity, which governs the loading of hydrokinetic turbine blades, varies both in  
8 space and time. The special variations of the river flow velocity are presented as the river velocity  
9 profile in the cross section of the river. The river flow velocity also fluctuates randomly over time.  
10 The river flow velocity should therefore be described by a time-dependent random field that varies  
11 randomly over space and time. The complicated properties of the river flow velocity, however, have  
12 brought great challenges to its measurements, especially for large rivers with depths exceeding  
13 several meters and with velocities greater than 1 m/s [22]. As a result, the information of the spatial  
14 variations of the river flow velocity is generally unavailable.

15 Fortunately, the river discharge data of many rivers are usually recorded and can be used to derive  
16 the statistical property of the average river flow velocity over the river cross section. For this reason,  
17 in this work, we only account for the average river flow velocity over the river cross section, and we  
18 then model the river flow velocity as a stochastic process. In other words, the spatial variation of the  
19 river flow velocity over location is neglected, and only its time variation is considered.

20 The other reasons of using a stochastic process for the river flow velocity are as follows: First, the  
21 hydrokinetic turbine system in this study is different from traditional hydropower plants. It is  
22 designed to be portable and is installed on a removable device, such as a vessel. This enables the  
23 turbine system to operate at different locations. It is difficult to predetermine at which location the

1 velocity should be used. Second, for large rivers where the hydrokinetic turbine is supposed to  
2 operate, the effect of the velocity profile in the cross section is smaller than that of small rivers. Third,  
3 the present work concentrates on the general time-dependent reliability analysis. The average river  
4 velocity model can be easily substituted by a maximal river flow velocity model when the  
5 corresponding statistical data are available.

6 According to the Manning-Strickler formula [23], given a site, the cross-section average river  
7 flow velocity is governed by the following equation [24-25]:

$$8 \quad v(t) = n^{-1} H(t)^{2/3} S^{1/2} \quad (1)$$

9 where  $v(t)$  is the river flow velocity [m/s],  $n$  is the river bed roughness,  $H(t)$  is the hydraulic  
10 radius [m], and  $S$  is the river slope [m/m].

11 With the assumption that the shape of river bed is a rectangle, the hydraulic radius  $H$  is  
12 presented in terms of the depth ( $D$  [m]) and width ( $W$  [m]) of the river flow as follows:

$$13 \quad H(t) = DW / (2D + W) \quad (2)$$

14 After carrying out research on a dataset of 674 river cross sections across the USA and Canada,  
15 Allen [26] found a relationship between the discharge, depth, and width with the following  
16 equations introduced by Leopold and Maddock [27]:

$$17 \quad W = 2.71 d_m^{0.557} \quad (3)$$

18 and

$$19 \quad D = 0.349 d_m^{0.341} \quad (4)$$

20 where  $d_m$  is the discharge of the river [m<sup>3</sup>/s].

21 From above equations, given the river bed roughness and river bed slope, the river velocity is  
22 associated with the river discharge. Therefore, the statistical characteristics of the river flow  
23 velocity are governed by those of the river flow discharge.

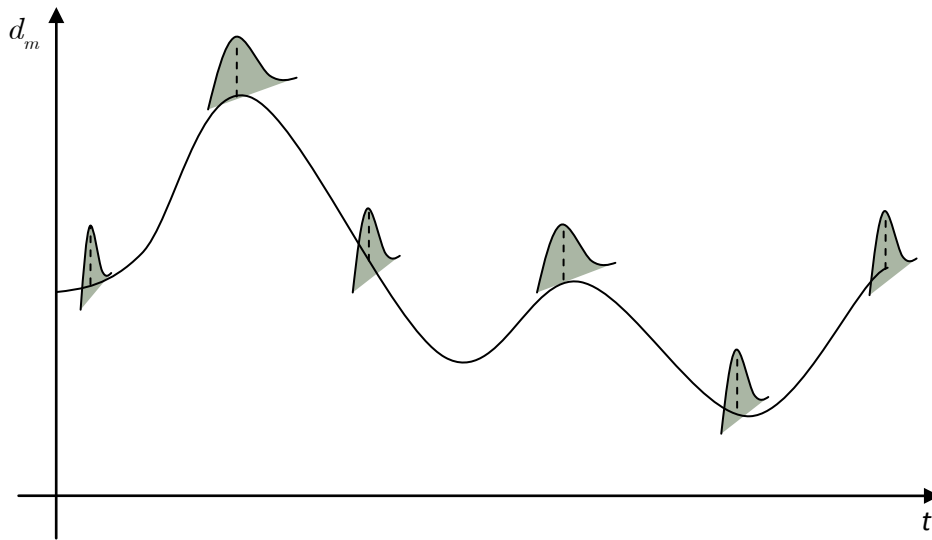
1 2.1.2 Statistical characteristics of river flow velocity

2 Since the fluctuation of river flow discharge is much smaller than that of the wind speed, we  
3 use the monthly river flow discharge to describe the river flow discharge climate. The monthly  
4 river discharge follows a lognormal distribution [28-34]. Therefore, the cumulative probability  
5 density function (CDF) of the monthly river discharge is given by

6 
$$F_{D_m}(d_m) = \Phi\{[\ln(d_m) - \mu_{D_m}(t)] / \sigma_{D_m}(t)\} \quad (5)$$

7 in which  $\mu_{D_m}(t)$  and  $\sigma_{D_m}(t)$  are the mean and standard deviation of  $\ln(d_m)$ , respectively,  $\Phi(\cdot)$   
8 is the CDF of a standard normal variable. Due to the seasonality of the river discharge,  $\mu_{D_m}(t)$   
9 and  $\sigma_{D_m}(t)$  are time dependent, and they vary in different months during a year. The river  
10 discharge in the time domain is, therefore, a stochastic process. As illustrated in Fig. 1, the river  
11 discharge follows a certain statistical distribution at each time instant, and the mean and standard  
12 deviation of the distribution vary over time.

13



14

15

**Fig. 1** Illustration of river discharge stochastic process



1 Besides, the monthly river discharge  $d_m$  at each time instant can be normalized and  
 2 standardized [14, 30, 35-37]. The coefficient of autocorrelation of the normalized and  
 3 standardized monthly river discharge is approximated by

$$4 \quad \rho_V(t_1, t_2) = \exp\left\{-[(t_2 - t_1) / \xi]^2\right\} \quad (6)$$

5 where  $\xi$  is the correlation length. Thus, the normalized and standardized monthly river  
 6 discharge is a Gaussian process with autocorrelation function in Eq. (6). The normalization and  
 7 standardization of the monthly river discharge will be discussed later.

8 In the above analysis, the cut-out river flow velocity  $V_c$  is not considered. When the river  
 9 velocity reaches the cut-out river flow velocity, the hydrokinetic turbine will shut down for a  
 10 safety reason. With such a cut-out velocity, the upper tail of the lognormal distribution of the  
 11 river discharge is truncated, and Eq. (5) becomes

$$12 \quad F_{D_m}(d_m) = F_{V_d}(d_m) / F_{V_d}(d_c) \\
 = \Phi\left\{[\ln(d_m) - \mu_{D_m}(t)] / \sigma_{D_m}(t)\right\} / \Phi\left\{[\ln(d_c) - \mu_{D_m}(t)] / \sigma_{D_m}(t)\right\} \quad (0 < d_m < d_c) \quad (7)$$

13 where  $d_c$  is the river discharge corresponding to the cut-out river flow velocity  $V_c$ , and  $F_{D_m}(d_m)$   
 14 is the CDF of the monthly river discharge  $d_m$ .

15 After obtaining the CDF of the monthly river discharge, we can also find the CDF of the  
 16 river flow velocity as indicated in Eq. (1). Thus, the statistical characteristics of the river flow  
 17 velocity are available with Eqs. (1) through (7).

18

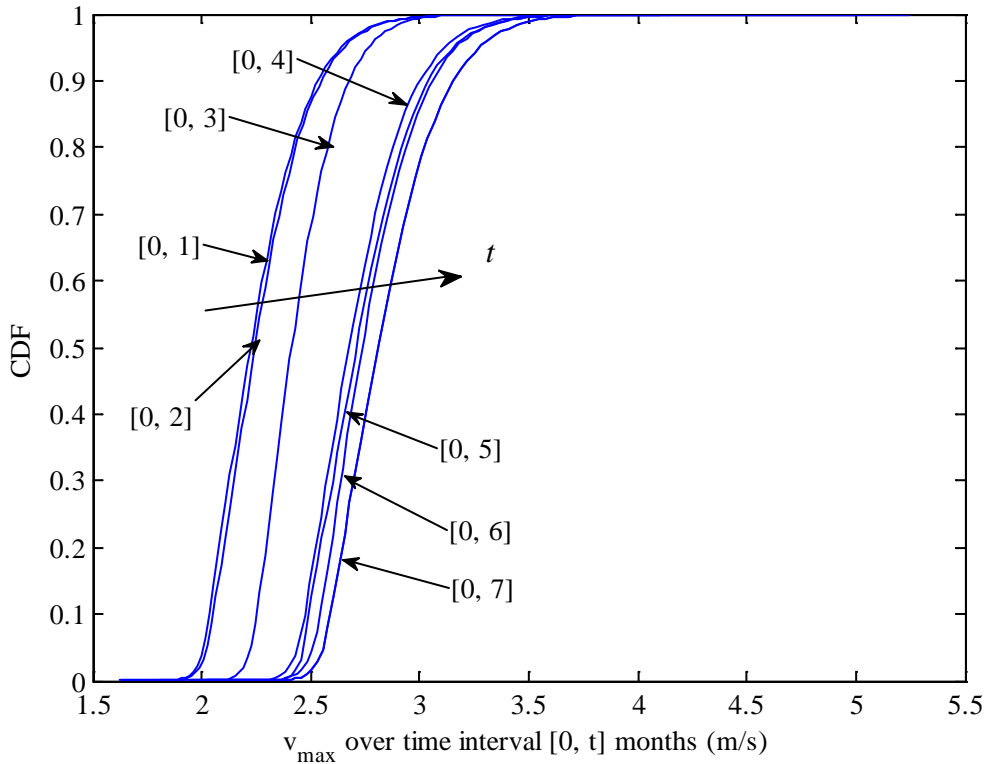
### 19 *2.1.3 Maximum velocity of the river*

20 Recall that the river discharge in the time domain is a stochastic process, the associated river  
 21 velocity in the time domain is a stochastic process as well. For a stochastic process, we are

1 interested in the extreme value of the process as it is directly related to the reliability of the  
 2 hydrokinetic turbine blades. If we discretized a time period  $[0, t]$  into  $n$  time instants and the  
 3 simulated river velocities at these time instants were  $v(t_i), i = 1, 2, \dots, n$ , the maximum velocity  
 4 over the time interval  $[0, t]$  would be

$$5 \quad v_{\max} = \max\{v(t_i), i = 1, 2, \dots, n\} \quad (8)$$

6 Since the river velocity is a random variable at each time instant, the maximum velocity  $v_{\max}$   
 7 is also a random variable with an unknown distribution. In addition to this, the longer is the time  
 8 period  $[0, t]$ , the higher is  $v_{\max}$ . Fig. 2 shows the simulated CDFs of the maximum velocities of  
 9 the Missouri river over different time periods.



10

11

**Fig. 2** CDFs of the maximum flow velocities

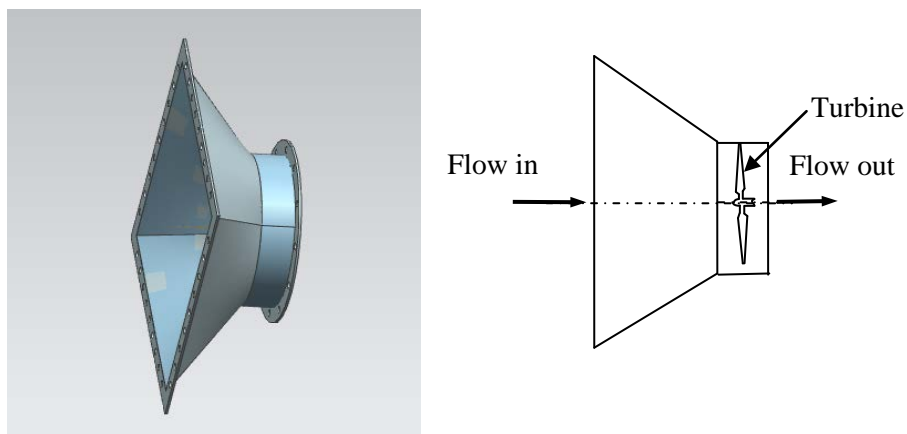
1 We see that the CDF curves of the maximum river velocities shift from left to right when the  
2 time period becomes longer. This implies that the hydrokinetic turbine blades have a higher  
3 probability of failure when the time interval becomes larger. For the time-dependent reliability  
4 analysis over different time intervals, different CDFs of the maximum river velocity are required.  
5 As the distribution of river velocity is non-Gaussian and the loading of the turbine blade is a non-  
6 linear response of the river velocity, we do not have explicit expression for the extreme loading  
7 on the turbine blades. If the simulation methods are employed to get the extreme loading of the  
8 turbine blades, the computational cost may not be affordable. To improve the efficiency, we will  
9 introduce an efficient time-dependent reliability analysis method for the hydrokinetic turbine  
10 blades in section 3.

11 In the following sections, we will discuss the relationship between the river velocity and the  
12 turbine blade loading response.

13

#### 14 *2.1.4 River flow velocity on the hydrokinetic turbine*

15 For a horizontal hydrokinetic turbine, a diffuser, as shown in Fig. 3, is typically used to  
16 increase the flow velocity that enters the turbine.



17

18

**Fig. 3** The diffuser for the horizontal hydrokinetic turbine

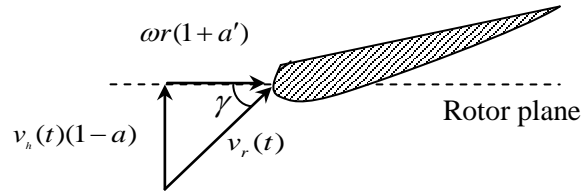
1 With the diffuser, the river velocity on the hydrokinetic turbine  $v_h$  is

$$2 \quad v_h(t) = C_{diffuser} v(t) \quad (9)$$

3 where  $C_{diffuser}$  is the velocity increasing coefficient of the diffuser. The value of  $C_{diffuser}$  is  
 4 dependent on the geometry of the diffuser.

### 6 2.1.5 River flow velocity analysis when turbine blades are rotating

7 In the above analysis, the rotation of hydrokinetic turbine is not taken into consideration.  
 8 When the hydrokinetic turbine is under operation, seen from the section of the turbine blade, the  
 9 relative velocity  $v_r$  acting on the turbine blades should be a combination of the axial velocity  
 10 and tangential velocity in the rotor plane [38]. The combination of velocities is shown in Fig. 4.



11

12 **Fig. 4** River flow velocity in the cross section of the turbine blade

13 The relative velocity acting on the turbine blade is given by

$$14 \quad v_r(t) = \sqrt{[v_h(t)(1-a)]^2 + [\omega r(1+a')]^2} \quad (10)$$

15 in which

$$16 \quad \omega = \lambda v_h(t) / R \quad (11)$$

17 where  $a$  is the axial induction factor,  $a'$  is the tangential induction factor,  $\omega$  is the angular  
 18 velocity of the rotor,  $r$  is the radial position of the control volume,  $\lambda$  is the tip speed ratio, and

1  $R$  is the radius of turbine blade. Besides, the optimal values of  $a$  and  $a'$  are related to the  
 2 chords, twist angles, pitch of the blade, and  $\omega r / V_h(t)$ .  $a$  and  $a'$  can be obtained from the blade  
 3 element momentum model [38], and Prandtl's and Glauert's corrections have been made for  $a$   
 4 and  $a'$  [39] in the blade element momentum codes.

## 6 2.2 Loading of hydrokinetic turbine blades

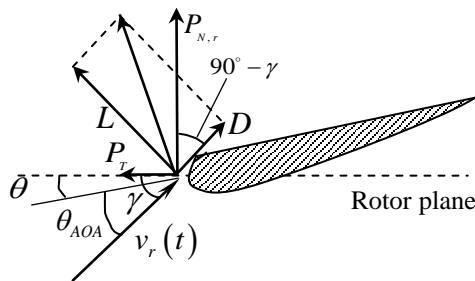
7 According to the blade element momentum theory, if the lift coefficient  $C_l$  and drag  
 8 coefficient  $C_d$  are known, the lift and drag forces per length are given by [38]

$$9 \quad L = \rho v_r(t)^2 c(r) C_l / 2 \quad (12)$$

10 and

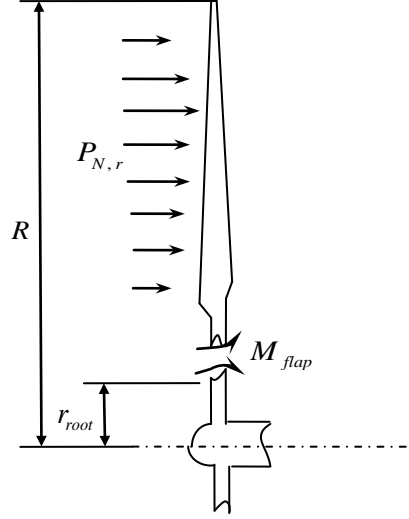
$$11 \quad D = \rho v_r(t)^2 c(r) C_d / 2 \quad (13)$$

12 respectively, where  $\rho$  is the water density, and  $c(r)$  is the chord at radius  $r$ ;  $C_l$  and  $C_d$  are  
 13 associated with the local angle of attack. Then the force of river flow acting on the blade can be  
 14 decomposed into two components  $P_T$  and  $P_N$ , which are normal and tangential to the rotor  
 15 plane, respectively. These forces are depicted in Fig. 5.



16  
 17 **Fig. 5** Forces of river flow

1 The normal force results in the flapwise bending moment at the root of a blade, as shown in  
 2 Fig. 6.



3

4

**Fig. 6** Bending moment on the turbine blade

5 The normal force per length, denoted by  $P_{N,r}$  at radius  $r$ , is given by [38]

$$\begin{aligned}
 P_{N,r}(t) &= L \cos \gamma + D \sin \gamma \\
 &= 0.5\rho \left( (v_h(t)(1-a))^2 + (\omega r(1+a'))^2 \right) (c(r)C_l \cos \gamma + c(r)C_d \sin \gamma)
 \end{aligned}
 \tag{14}$$

6

7 where  $\gamma$  is the flow angle, which is the summation of the local angle of attack  $\theta_{AOA}$  and the

8 local pitch  $\theta$ . The local pitch  $\theta$  is the combination of the pitch angle  $\theta_p$  and twist angle  $\theta_t(r)$

9 of the blade. The flow angle is determined by the following equation:

$$\tan \gamma = [(1-a)v_h(t)] / [(1+a')\omega r] = (1-a)R / [(1+a')\lambda r]
 \tag{15}$$

10

11 After obtaining the flow angle, we can calculate the angle of attack at radius  $r$  by

$$\theta_{AOA} = \gamma - (\theta_p + \theta_t(r))
 \tag{16}$$

12

13 Then with the angle of attack,  $C_l$  and  $C_d$  at radius  $r$  can be calculated according to the

14 airfoil's characteristics.

1 From Eqs. (9), (14) and (15), we have

$$2 \quad P_{N,r}(t) = 0.5\rho v^2(t)C_{diffuser}^2 \left( (1-a)^2 + r^2\lambda^2(1+a')^2 / R^2 \right) \left( c(r)C_l \cos \gamma + c(r)C_d \sin \gamma \right) \quad (17)$$

3 Let

$$4 \quad C_1(r) = C_{diffuser}^2 \left( (1-a)^2 + r^2\lambda^2(1+a')^2 / R^2 \right) \quad (18)$$

$$5 \quad C_2(r) = \left( c(r)C_l \cos \gamma + c(r)C_d \sin \gamma \right) \quad (19)$$

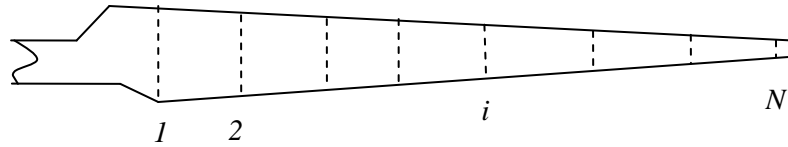
6 With a fixed tip speed ratio  $\lambda$ , Eq. (17) is rewritten as

$$7 \quad P_{N,r}(t) = 0.5\rho v^2(t)C_1(r)C_2(r) \quad (20)$$

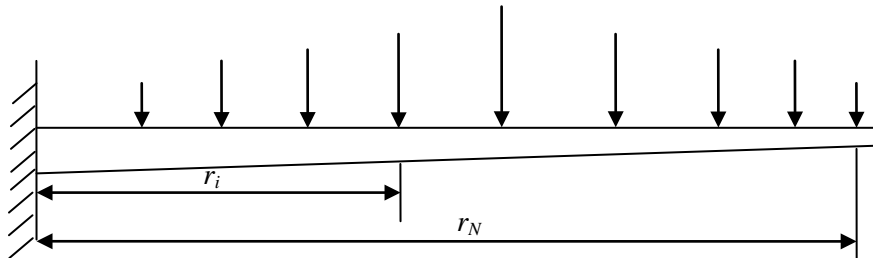
8 Substituting Eqs. (1) through (4) into Eq. (20) yields

$$9 \quad P_{N,r}(t) = 0.5\rho \left( 2.71d_m^{0.557} / (2 + 7.765d_m^{0.216}) \right)^{4/3} SC_1(r)C_2(r) / n^2 \quad (21)$$

10 In order to calculate the bending moment at the root of the blade, we divide the blade into  $N$   
 11 segments as shown in Fig. 7 (a). The blade can be further simplified as shown in Fig. 7 (b).



14 (a) Segments of the hydrokinetic turbine blade



17 (b) Simplified turbine blade loading model

18 **Fig. 7** Normal forces on the hydrokinetic turbine blade

1 Based on the assumption of a linear variation of the load, the flapwise bending moment at the  
 2 root of the blade can be computed by [38]

$$3 \quad M_{flap}(t) = \sum_{i=1}^{N-1} \left( \frac{1}{3} \left( \frac{P_{N,r_{i+1}}(t) - P_{N,r_i}(t)}{r_{i+1} - r_i} \right) (r_{i+1}^3 - r_i^3) + \frac{1}{2} \left( \frac{P_{N,r_i}(t)r_{i+1} - P_{N,r_{i+1}}(t)r_i}{r_{i+1} - r_i} \right) (r_{i+1}^2 - r_i^2) \right) \quad (22)$$

4 where  $M_{flap}$  is the flapwise bending moment,  $r_{i+1} = r_{root} + (R - r_{root})i / N$ , and  $r_{root}$  is the  
 5 radius of the hub.

6 Substituting Eq. (21) into Eq. (22), we obtain the flapwise bending moment at the root of the  
 7 blade

$$8 \quad M_{flap}(t) = 0.5\rho \left( 2.71d_m^{0.557} / (2 + 7.765d_m^{0.216}) \right)^{4/3} SC_{sum} / n^2 \quad (23)$$

9 in which

$$10 \quad C_{sum} = \sum_{i=1}^{N-1} \left( \left( [C_1(r_{i+1})C_2(r_{i+1}) - C_1(r_i)C_2(r_i)] / (r_{i+1} - r_i) \right) (r_{i+1}^3 - r_i^3) / 3 \right. \\ \left. + \left( [C_1(r_i)C_2(r_i)r_{i+1} - C_1(r_{i+1})C_2(r_{i+1})r_i] / (r_{i+1} - r_i) \right) (r_{i+1}^2 - r_i^2) / 2 \right) \quad (24)$$

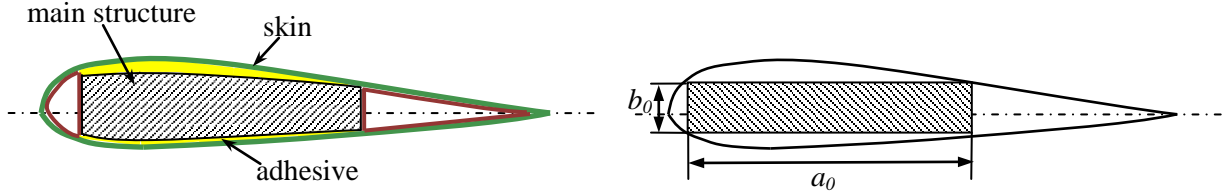
## 11 12 **2.3 Material resistance**

13 Due to the variability of blade materials, their strength should be characterized by a certain  
 14 probability distribution. Similar to the work on the reliability analysis of steel structure [40-41],  
 15 we assume that the distribution of the yield strength,  $m_s$ , of the blade material, follows a normal  
 16 distribution with mean  $\mu_s$  and standard deviation  $\sigma_s$ ; namely  $m_s \sim N(\mu_s, \sigma_s)$ .

17 In order to compute the maximum bending moment that the material can resist at the root of  
 18 the blade, we simplify the cross section of the turbine blade as shown in Fig. 8. As for a  
 19 hydrokinetic turbine blade, a thin skin is glued on a box-like structure (the main structure) to  
 20 define the geometry, as shown on the left of Fig. 8. Since the shape of the main structure is



1 almost rectangular, we can simplify the cross section as a rectangle, as shown on the right of Fig.  
 2 8. Given the box-like structure, the error of the assumption of the rectangular cross section is  
 3 acceptable for the root section.



4  
 5 **Fig. 8** Simplified cross section of the hydrokinetic turbine blade

6 The allowable bending moment can thus be obtained by

$$7 \quad M_{allow} = m_s a_0 b_0^2 / 4 \quad (25)$$

8 where  $a_0$  and  $b_0$  are the width and height of the blade after simplification, respectively. They are  
 9 random variables due to the tolerance of manufacturing and clearance of assembly.

10  
 11 **2.4 Limit-state function for turbine blade reliability analysis**

12 For hydrokinetic turbine blades, the bending moment should not exceed the allowable  
 13 bending moment in Eq. (25). Based on this, applying Eqs. (23) through (25), we define the limit-  
 14 state function as follows:

$$15 \quad g(\mathbf{X}, \mathbf{Y}(t), t) = M_{flap}(t) - M_{allow}(t) \quad (26)$$

16 where  $\mathbf{X}$  is the vector of random variables, and  $\mathbf{Y}(t)$  is the vector of stochastic processes. In this  
 17 problem,  $\mathbf{X} = \{a_0, b_0, m_s\}$  and  $\mathbf{Y}(t)$  has only one element, which is the monthly discharge  $d_m$ .

1  $M_{flap}(t)$  is the flapwise bending moment given in Eq. (23), and  $M_{allow}(t)$  is the allowable  
2 bending moment given in Eq. (25). When  $g(\mathbf{X}, \mathbf{Y}(t), t) > 0$ , a failure occurs.

3

### 4 **3. Reliability analysis**

5 For the reliability analysis of hydrokinetic turbine blades, we assume that the seasonal effects  
6 repeat in the same time periods of any year. This assumption is based on the fact that the Earth  
7 circulates around the Sun annually with the same seasonal effects. The yearly river climates,  
8 therefore, are independent with the same seasonality. The probability of failure during a  $T$ -year  
9 operation can be calculated as

$$10 \quad p_f(T) = 1 - [1 - p_f(Y_e)]^T \quad (27)$$

11 where  $p_f(T)$  is the probability of failure during  $T$  years;  $p_f(Y_e)$  is the yearly probability of  
12 failure.

13 Consequently, the yearly probability of failure of the turbine blade should be calculated first.  
14 Calculating  $p_f(Y_e)$  requires time-dependent reliability analysis.

15

### 16 **3.1 Time-dependent reliability analysis**

#### 17 *3.1.1 Time-dependent reliability analysis with upcrossing rate*

18 The above mentioned yearly probability of failure  $p_f(Y_e)$  is defined over a time interval  
19  $[0, t]$ , where  $t$  is equal to one year.  $p_f(Y_e)$  is a time-dependent probability of failure, and a  
20 general form of the time-dependent probability of failure over time period  $[t_0, t_e]$  is defined as

1 
$$p_f(t_0, t_e) = \Pr \left\{ Z(\tau) = g(\mathbf{X}, \mathbf{Y}(\tau), \tau) > e(\tau), \tau \in [t_0, t_e] \right\} \quad (28)$$

2 where  $t_0$  is the initial time of operation, and  $t_e$  is the end point of the evaluated time period.  $e(\cdot)$   
 3 is a time-dependent limit state, and  $\Pr\{\cdot\}$  stands for a probability.

4 With the integration of the Poisson assumption based upcrossing rate method and the First  
 5 Order Reliability Method (FORM),  $p_f(t_0, t_s)$  is calculated by [21, 42]

6 
$$p_f(t_0, t_s) = 1 - [1 - p_f(t_0)] \exp \left\{ - \int_{t_0}^{t_s} v^+(t) dt \right\} \quad (29)$$

7 where  $v^+(t)$  is the upcrossing rate at  $t$ ,  $p_f(t_0)$  is the instantaneous probability of failure at the  
 8 initial time point  $t_0$ . An instantaneous probability of failure  $p_f(t)$  is the likelihood of failure at a  
 9 particular time instant  $t$  and is calculated by

10 
$$p_f(t) = \Pr \left\{ g(\mathbf{X}, \mathbf{Y}(t), t) > e(t) \right\} \quad (30)$$

11 The instantaneous probability of failure can be solved with FORM. The equation for solving  
 12 the instantaneous probability of failure will be given in the next section. Once we have the  
 13 upcrossing rate  $v^+(t)$ , the time-dependent probability of failure  $p_f(t_0, t_s)$  can be calculated by  
 14 integrating  $v^+(t)$  over  $[t_0, t_e]$ .

15 Apparently, the key for calculating  $p_f(t_0, t_s)$  with Eq. (29) is the computation of the  
 16 upcrossing rate  $v^+(t)$ . In the following subsections, we first review how to obtain the upcrossing  
 17 rate by using FORM and the Rice's formula. We then discuss how to apply this method to the  
 18 time-dependent reliability analysis of hydrokinetic turbine blades.

19

1 3.1.2 Upcrossing rate  $v^+(t)$

2 For a general limit-state function  $Z(t) = g(\mathbf{X}, \mathbf{Y}(t), t)$  given in Eq. (28), at a time instant  $t$ ,  
 3 its random variables and stochastic processes  $(\mathbf{X}, \mathbf{Y}(t))$  are transformed into the standard normal  
 4 random variables  $\mathbf{U}(t) = (\mathbf{U}_x, \mathbf{U}_y(t))$ . After the transformation, the limit-state function is  
 5 linearized at the Most Probable Point (MPP)  $\mathbf{U}^*(t)$ , which is a point at the limit state, and at this  
 6 point the limit-state function has the highest probability density. Then at the MPP, the probability  
 7 of failure is equivalent to

8 
$$\Pr\{L(t) = \boldsymbol{\alpha}(t)\mathbf{U}(t)^T > \beta(t), t \in [t_0, t_e]\}$$
 (31)

9 where

10 
$$\boldsymbol{\alpha}(t) = \nabla \mathbf{g}(\mathbf{U}^*(t), t) / \|\nabla \mathbf{g}(\mathbf{U}^*(t), t)\|$$
 (32)

11  $\beta(t)$  is the reliability index, which is the length of  $\mathbf{U}^*(t)$ ; and  $\|\cdot\|$  stands for the length of a vector.

12 Besides, the reliability index is used to calculate the instantaneous probability of failure at a time  
 13 instant  $t_i$  as follows:

14 
$$p_f(t_i) = 1 - \Phi(\beta(t_i))$$
 (33)

15 The above equation can also be used to calculate the initial instantaneous probability of  
 16 failure  $p_f(t_0)$  in Eq. (29).

17 From Eq. (32), we have  $\|\boldsymbol{\alpha}(t)\| = 1$ , and  $L(t)$  is therefore a standard normal stochastic  
 18 process. Then the uncrossing rate  $v^+(t)$  can be calculated using the Rice's formula [43-44] as  
 19 follows:

1 
$$v^+(t) = \omega(t) \phi(\beta(t)) \Psi(\dot{\beta}(t) / \omega(t)) \quad (34)$$

2 where  $\Psi(\cdot)$  is a function defined by

3 
$$\Psi(x) = \phi(x) - x\Phi(-x) \quad (35)$$

4  $\omega^2(t)$  is given in terms of the correlation function  $\rho(t_1, t_2)$  of  $L(t)$  as follows:

5 
$$\omega^2(t) = \partial^2 \rho(t, t) / \partial t_1 \partial t_2 \quad (36)$$

6 Since  $L(t)$  is a standard normal stochastic process, its coefficient of correlation is given by

7 
$$\rho(t_1, t_2) = \boldsymbol{\alpha}(t_1) \mathbf{C}(t_1, t_2) \boldsymbol{\alpha}(t_2)^T \quad (37)$$

8 where  $\mathbf{C}(t_1, t_2)$  is the covariance matrix of  $L(t_1)$  and  $L(t_2)$  and has the following form:

9 
$$\mathbf{C}(t_1, t_2) = \begin{bmatrix} \mathbf{I}_{n \times n} & 0 \\ 0 & \mathbf{C}^Y(t_1, t_2) \end{bmatrix} \quad (38)$$

10 where  $\mathbf{I}_{n \times n}$  is an  $n \times n$  identity matrix, which is the covariance matrix of the normalized random  
 11 variables  $\mathbf{U}_X$  for  $\mathbf{X}$ , and  $\mathbf{C}^Y(t_1, t_2)$  is the covariance matrix of the normalized stochastic process  
 12  $\mathbf{U}_Y(t)$ . In this problem, the covariance matrix just has one element, which is the covariance of  
 13 the normalized river discharge stochastic process.

14 Given the correlation coefficients of the normalized stochastic process  $\mathbf{U}_Y(t)$ , the covariance  
 15 matrix  $\mathbf{C}^Y(t_1, t_2)$  is presented as

16 
$$\mathbf{C}^Y(t_1, t_2) = \begin{bmatrix} C^{Y_1}(t_1, t_2) & 0 & \cdots & 0 \\ 0 & \ddots & \cdots & 0 \\ \vdots & \vdots & \ddots & \vdots \\ 0 & 0 & \cdots & C^{Y_m}(t_1, t_2) \end{bmatrix} = \begin{bmatrix} \rho^{Y_1} & 0 & \cdots & 0 \\ 0 & \ddots & \cdots & 0 \\ \vdots & \vdots & \ddots & \vdots \\ 0 & 0 & \cdots & \rho^{Y_m} \end{bmatrix} \quad (39)$$

17 where  $C^{Y_i}(t_1, t_2)$  is the covariance of the normalized stochastic process  $U_{Y_i}(t)$  at time instants  $t_1$

18 and  $t_2$ .  $\rho^{Y_i}$  is the corresponding correlation function and is given by

$$\rho^{Y_i} = \rho^{Y_i}(t_1, t_2) \quad (40)$$

In this problem, the correlation of river discharge at two time instants can be obtained from Eq. (6).

Then substituting Eq. (37) into Eq. (36), we have

$$\omega(t)^2 = \dot{\alpha}(t)\dot{\alpha}(t)^T + \alpha(t)\ddot{\mathbf{C}}_{12}(t, t)\alpha(t)^T \quad (41)$$

in which

$$\ddot{\mathbf{C}}_{12}(t, t) = \begin{pmatrix} \mathbf{0} & 0 \\ 0 & \ddot{\mathbf{C}}_{12}^{Y_i}(t, t) \end{pmatrix} \quad (42)$$

and

$$C_{12}^{Y_i}(t, t) = \partial^2 \rho^{Y_i}(t, t) / \partial t_1 \partial t_2, i = 1, 2, \dots, m \quad (43)$$

where  $m$  is the number of stochastic processes. For the turbine blade problem,  $m=1$ .

$\dot{\alpha}(t)$  and  $\dot{\beta}(t)$  are required as indicated in Eq. (34) and Eq. (41). Because we use the finite difference method to calculate the derivatives, we need to carry out two MPP searches at every time instants  $t$  and  $t + \Delta t$ , where  $\Delta t$  is a small step size. The derivatives are given by

$$\dot{\alpha}(t) = [\alpha(t + \Delta t) - \alpha(t)] / \Delta t \quad (44)$$

and

$$\dot{\beta}(t) = [\beta(t + \Delta t) - \beta(t)] / \Delta t \quad (45)$$

Now all the equations are available for the upcrossing rate  $v^+(t)$  in Eq. (29). If we know  $\alpha(t)$  and  $\beta(t)$  of the limit-state function of hydrokinetic turbine blades, we can then calculate its yearly probability of failure  $p_f(Y_e)$  using Eqs. (29) through (45).

### 3.2 Time-dependent reliability analysis for hydrokinetic turbine blades

In this section, we use the time-dependent reliability analysis method presented above to solve for the probability of failure of hydrokinetic turbine blades. We first discuss the

1 transformation of the non-Gaussian random variable  $(\mathbf{X}, \mathbf{Y}(t))$  into standard Gaussian random  
 2 variable  $\mathbf{U}(t) = (\mathbf{U}_x, \mathbf{U}_y(t))$ . Based on this, we then provide the approach of obtaining  $\alpha(t)$   
 3 and  $\beta(t)$  required by Eqs. (34) through (45) for time-dependent reliability analysis.

4

### 5 3.2.1 Transform non-Gaussian random variables

6 Due to the cut-out river flow velocity, a non-Gaussian random variable is involved. The non-  
 7 Gaussian random variable is the truncated lognormal random variable (the truncated monthly  
 8 river discharge). We need to transform it into equivalent normal distribution. The transformation  
 9 is given by

$$10 \quad U_{d_m} = [\ln(d_m) - \mu_{D_m}(t)] / \sigma_{D_m}(t) \sim N(0, 1) \quad (46)$$

11 where

$$12 \quad \sigma_{D_m}(t)^2 = \ln \left[ \left( \sigma_{d_m}(t) / \mu_{d_m}(t) \right)^2 + 1 \right] \quad (47)$$

13 and

$$14 \quad \mu_{D_m}(t) = \ln \left( \mu_{d_m}(t) \right) - 0.5 \sigma_{D_m}(t)^2 \quad (48)$$

15 After the truncation, the transformation becomes

$$16 \quad \tilde{U}_{d_m} = \Phi^{-1} \left( \Phi \left\{ [\ln(d_m) - \mu_{D_m}(t)] / \sigma_{D_m}(t) \right\} / \Phi \left\{ [\ln(d_c) - \mu_{D_m}(t)] / \sigma_{D_m}(t) \right\} \right) \quad (0 < d_m < d_c) \quad (49)$$

17

### 18 3.2.2 Solve for $\alpha(t)$ and $\beta(t)$

19 Recall that the limit-state function of the hydrokinetic turbine blade is

$$20 \quad g(\mathbf{X}, \mathbf{Y}(t), t) = 0.5 \rho \left( 2.71 d_m^{0.557} / (2 + 7.765 d_m^{0.216}) \right)^{4/3} SC_{sum} / n^2 - m_s a_0 b_0^2 / 4 \quad (50)$$

21 where  $C_{sum}$  is given in Eq. (24).

1 After the transformation, the limit-state function in Eq. (50) becomes

$$\begin{aligned}
 2 \quad & g(\mathbf{X}, \mathbf{Y}(t), t) = g(\mathbf{U}(t), t) \\
 & = 0.5\rho \left( 2.71 \cdot T(\tilde{U}_{d_m})^{0.557} / (2 + 7.765T(\tilde{U}_{d_m})^{0.216}) \right)^{4/3} SC_{sum} / n^2 - 0.25T(U_{a_0})T(U_{b_0})^2T(U_{m_s}) \quad (51)
 \end{aligned}$$

3 where  $T(\cdot)$  is the operator of transforming non-Gaussian random variables  $(\mathbf{X}, \mathbf{Y}(t))$  into  
 4 Gaussian random variables  $\mathbf{U}(t)$ .

5 Then, the MPP  $\mathbf{U}^*(t)$  at a given time instant  $t$  can be obtained by solving

$$\begin{cases}
 6 \quad \min \beta(t) = \|\mathbf{u}(t)\| \\
 \text{s.t. } g(\mathbf{u}(t), t) = 0
 \end{cases} \quad (52)$$

7 After obtaining the MPP  $\mathbf{u}^*(t)$  at a given time instant  $t$ , we get  $\alpha(t)$  and  $\beta(t)$  as follows:

$$8 \quad \beta(t) = \|\mathbf{U}^*(t)\| \quad (53)$$

9 and

$$10 \quad \alpha(t) = -\mathbf{U}^*(t) / \|\mathbf{U}^*(t)\| \quad (54)$$

11 Similarly, we can also solve for the  $\alpha(t + \Delta t)$  and  $\beta(t + \Delta t)$ , which are then used to  
 12 calculate  $\dot{\alpha}(t)$  and  $\dot{\beta}(t)$  in Eqs. (34) and (41). The yearly probability of failure  $p_f(Y_e)$  is then  
 13 solved with Eqs. (29) through (45). And the probability of failure during  $T$ -year operation,  $p_f(T)$ ,  
 14 is finally obtained with Eq. (27).

15

### 16 3.3 Sensitivity analysis of random variables

17 The time-dependent reliability analysis not only provides the likelihood of failure over a time  
 18 period but also helps us understand how random variables affect such likelihood. The latter is  
 19 achieved by sensitivity analysis. Sensitivity analysis shows the relative importance of each  
 20 random variable to the probability of failure [45]. The sensitivities of random variables are



1 represented by the sensitivity factors [46]. Since the limit-state function  $g(\mathbf{X}, \mathbf{Y}, t)$  has been  
 2 transformed into  $g(\mathbf{U}, t)$ , the sensitivity factor  $\varepsilon_i(t)$  with respect to a random variable  
 3  $U_i$  ( $i = 1, 2, \dots, 4$ ) can be determined by

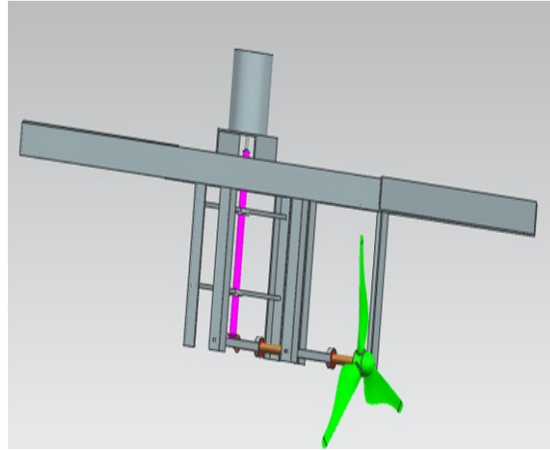
$$\begin{aligned}
 \varepsilon_i(t) &= -\partial\beta(t) / \partial U_i = -\partial[\sum_{i=1}^4 (U_i^*)^2]^{0.5} / \partial U_i^* \\
 &= -U_i^* / [\sum_{i=1}^4 (U_i^*)^2]^{0.5} = -U_i^* / \beta(t)
 \end{aligned}
 \tag{55}$$

5 Based on the sensitivity analysis of random variables at different instants of time, we can  
 6 determine their importance on the failure of the turbine blade. Besides, the change of the  
 7 importance of random variables over time period can also be evaluated. For important random  
 8 variables identified by sensitivity analysis, we should focus on effective ways to quantify their  
 9 uncertainties and identify their optimal distribution parameters during the design stage so that the  
 10 probability of failure can be maintained at a desired level with a reduced cost.

11

#### 12 **4. Example**

13 As mentioned previously, this work focuses on a hydrokinetic turbine with three one-meter  
 14 long rotor blades, fixed pitch angle, and tip speed ratio, developed for the operation in the  
 15 Missouri River. The sketch of the turbine is shown in Fig. 9. Its prototype under testing in a  
 16 water tunnel is shown in Fig. 10. The reliability of the hydrokinetic turbine over a 20-year design  
 17 period was evaluated.



1

2

**Fig. 9** 3-D modeling of a three blade hydrokinetic turbine



3

4

**Fig. 10** A horizontal-axis hydrokinetic turbine with three blades under testing

5

#### 6 **4.1. Data**

7 The deterministic variables and distributions of the random variables are given in Tables 1 and

8 2, respectively. In order to calculate the parameters related to the geometry of the hydrokinetic

9 turbine blade, we divided the blade into 30 segments. Assume that the turbine blade uses the

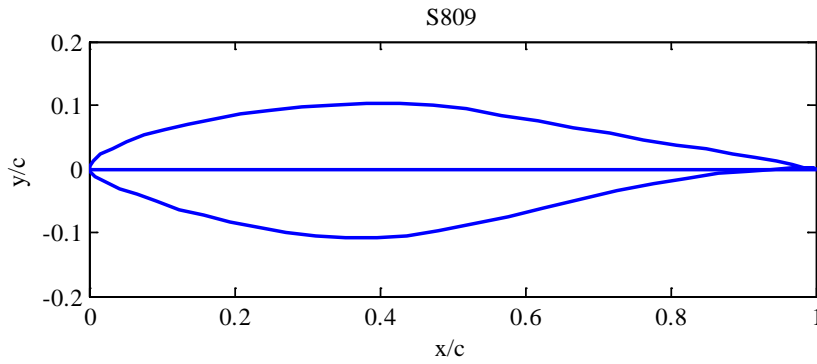
10 NREL S809 airfoil section, which is shown in Fig. 11. The corresponding data of lift and drag

11 coefficients were from [47]. The reason of using the NREL S809 airfoil for this example is that

1 it has been widely studied by many researchers and that reliable lift and drag coefficients are  
 2 available. The turbine blades are designed to have a 1 m radius with nonlinear chord length and  
 3 twist angle distributions, which use the NREL S809 airfoil from root to tip. The optimized chord  
 4 and twist angle distributions at different radii are plotted in Figs. 12 and 13, respectively. It is  
 5 noted that the reliability analysis method in this paper can also handle other kinds of airfoil  
 6 sections.

7 Table 1 Deterministic variables of the turbine blade problem

Variable	$\rho$	$\lambda$	$r_{root}$	$C_{diffuser}$	$V_C$	$\theta_p$	$R$	$n$	$S$
Value	$1 \times 10^3 \text{ kg/m}^3$	3	0.2 m	2	3.7 m/s	$6^\circ$	1 m	0.025	$4 \times 10^{-4} \text{ m/m}$

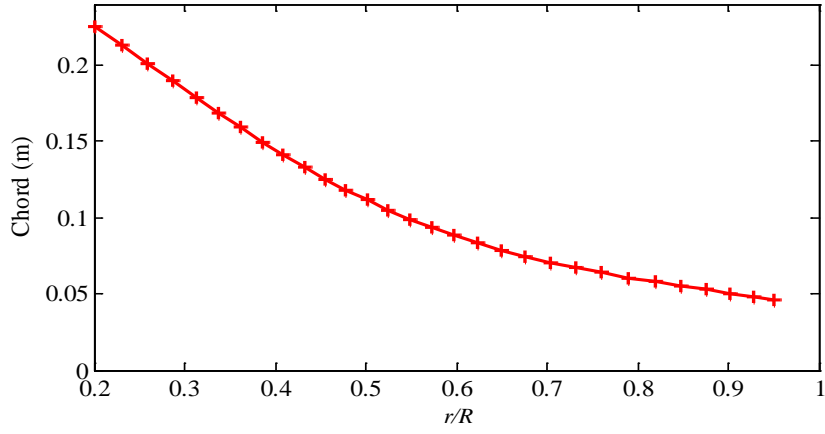


8  
9 **Fig. 11** NREL S809 airfoil profile

10 Table 2 Distribution of random variables of the turbine blade problem

Variable	Mean	Standard deviation	Distribution
$d_m$	$\mu_{d_m}(t)$	$\sigma_{d_m}(t)$	Lognormal
$a_0$	0.21 m	$1 \times 10^{-4} \text{ m}$	Normal
$b_0$	0.025 m	$1 \times 10^{-5} \text{ m}$	Normal
$\sigma_s$	$3.15 \times 10^5 \text{ kPa}$	$1.5 \times 10^4 \text{ kPa}$	Normal

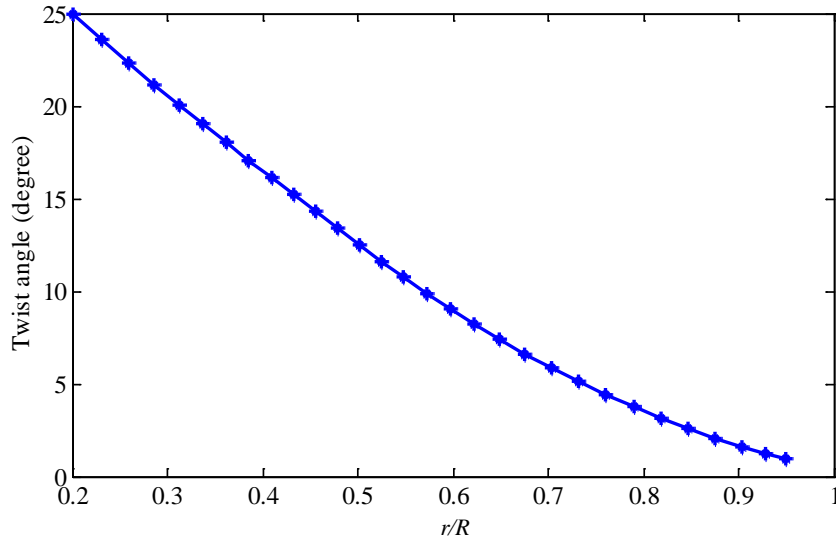
11



1

2

**Fig. 12** Chords distribution along the radius of the turbine blade



3

4

**Fig. 13** Twist angle distribution along the radius of the turbine blade

5

6

7

The historical river discharge data of the Missouri River from 1897 to 1988 at the Hermann, Missouri station [48] were used . Based on these data, we fitted the mean and standard deviation of the monthly river discharge as functions of  $t$  as follows:

8

$$\mu_{D_m}(t) = a_0^m + \sum_{i=1}^5 [a_i^m \cos(i\omega_m t) + b_i^m \sin(i\omega_m t)] \quad (56)$$

$$\sigma_{D_m}(t) = a_0^s + \sum_{j=1}^5 [a_j^s \cos(j\omega_s t) + b_j^s \sin(j\omega_s t)] \quad (57)$$

2 where

$$\begin{aligned} a_0^m = 2335, a_1^m = -1076, a_2^m = 241.3, a_3^m = 61.69, a_4^m = -30.92, a_5^m = 32.38, \\ b_1^m = 57.49, b_2^m = -174.9, b_3^m = -296.2, b_4^m = 213.6, b_5^m = -133.6, \omega_m = 0.5583 \end{aligned} \quad (58)$$

$$\begin{aligned} a_0^s = 1280, a_1^s = -497.2, a_2^s = 145.8, a_3^s = 225.4, a_4^s = -203.1, a_5^s = 99.47, \\ b_1^s = -82.58, b_2^s = -19.06, b_3^s = -178.7, b_4^s = 36.15, b_5^s = -52.47, \omega_s = 0.5887 \end{aligned} \quad (59)$$

5 These functions were selected as the ones that give the best fits to measurement data  
6 available. Besides, according to the “over time” autocorrelation function of the Elbe River at Neu  
7 Darchau [30], the autocorrelation coefficient function of the monthly discharge of Missouri river  
8 is assumed to be

$$\rho_{D_m}(t_1, t_2) = \exp\{-[6(t_2 - t_1) / 5]^2\} \quad (60)$$

## 11 4.2. Reliability analysis

12 By using the classical blade element momentum theory, the axial induction factor  $a$  and the  
13 tangential induction factor  $a'$  at different radii were computed first. Then the geometry related  
14 parameter  $C_{sum}$  was obtained from Eqs. (18), (19), and (24). After substituting the deterministic  
15 variables into Eq. (50), we obtained the limit-state function

$$g(\mathbf{X}, \mathbf{Y}(t), t) = 275.21 \left( 2.71 d_m^{0.557} / (2 + 7.765 d_m^{0.216}) \right)^{4/3} - a_0 b_0^2 m_s / 4 \quad (61)$$

17 The reliability analysis for the hydrokinetic turbine blade, was conducted with the following  
18 steps: First, the probability of failure of the hydrokinetic turbine blades without a cut-out velocity  
19 in a one-year time period  $[t_0, t_e] = [0, 1]$  yr was analyzed by using the time-dependent reliability  
20 analysis method. Since the yearly probabilities of failure were assumed to be independent, then

1 the probability of failure over the time life  $[t_0, t_e] = [0, 20]$  yr was computed using Eq. (27).  
2 Finally, in order to study the effect of cut-out velocity on reliability, we performed reliability  
3 analysis for the turbine blade with different cut-out river velocities. Meanwhile, as a byproduct  
4 of time-dependent reliability analysis, the sensitivities of random variables over time, were also  
5 obtained.

6

### 7 **4.3. Results and discussions**

#### 8 *4.3.1 Time-dependent reliability analysis results*

9 Table 3 shows the results of the probabilities of failure obtained from the time-dependent  
10 reliability analysis method. The solution from Mento Carlo Simulation (MCS) with a sample  
11 size of  $1 \times 10^6$  are also presented in Table 3 and plotted in Fig. 14.

12 MCS is a simulation method, which can estimate the probability of failure accurately when the  
13 sample size is large enough. For the stochastic process (the monthly river flow discharge), we  
14 used the Expansion Optimal Linear Estimation method (EOLE) [49-50] to generate the samples  
15 for the river flow discharge.

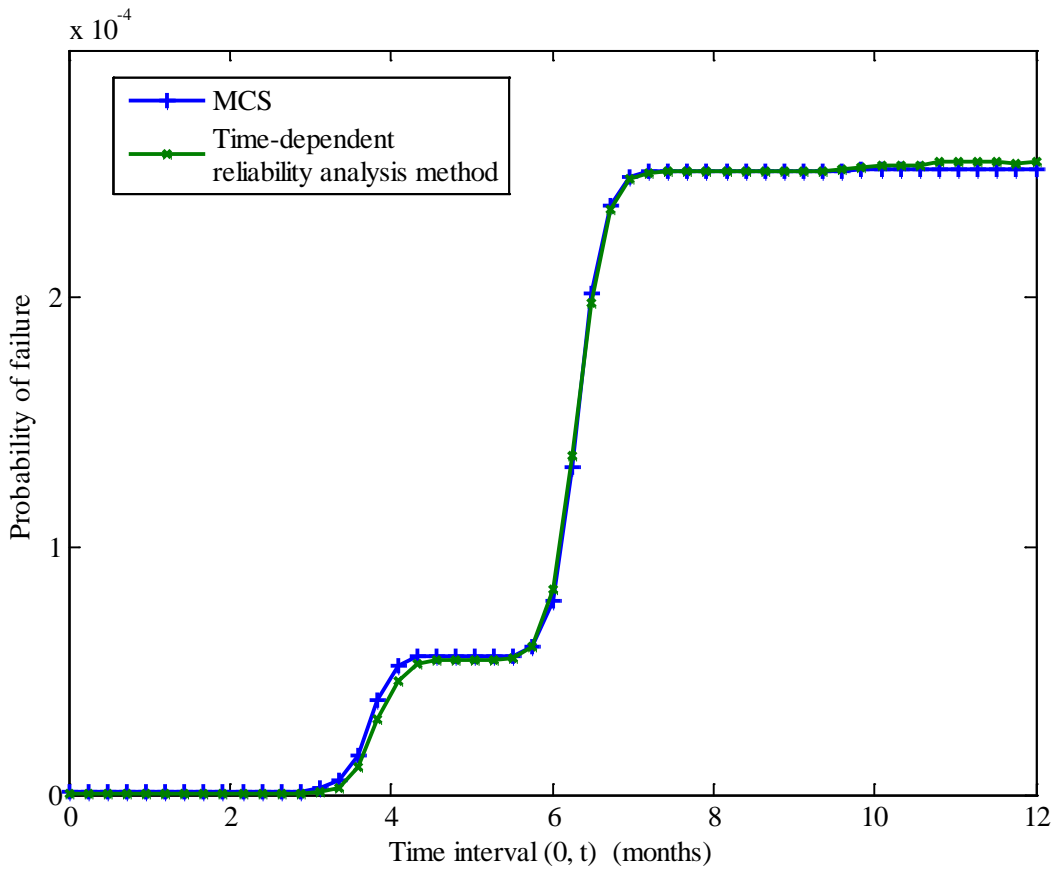
16 The results indicate the good accuracy of the reliability analysis method for the hydrokinetic  
17 turbine blade presented. Fig. 14 and Table 3 show that the time-dependent probability of failure  
18 of hydrokinetic turbine blades increases with time over a one-year time period. The probability  
19 of failure is  $2.546 \times 10^{-4}$  over a one-year period after the hydrokinetic turbine is put into operation.  
20 The probability of failure of the hydrokinetic turbine blades over its 20-year operation, or over  
21  $[t_0, t_e] = [0, 20]$  yr, is about  $5.1 \times 10^{-3}$ , which is obtained by substituting the yearly probability of  
22 failure  $2.546 \times 10^{-4}$  into Eq. (26).

1

Table 3  $p_f(t_0, t)$  of the hydrokinetic turbine blade over different time period

Time period (months)	$p_f(t_0, t)$	
	Time dependent ( $\times 10^{-4}$ )	MCS solution ( $\times 10^{-4}$ )
[0, 1]	0.006	0.010
[0, 2]	0.006	0.010
[0, 3]	0.029	0.060
[0, 4]	0.525	0.560
[0, 5]	0.544	0.560
[0, 6]	1.366	1.320
[0, 7]	2.508	2.510
[0, 8]	2.510	2.510
[0, 9]	2.509	2.510
[0, 10]	2.537	2.520
[0, 11]	2.546	2.520
[0, 12]	2.546	2.520

2



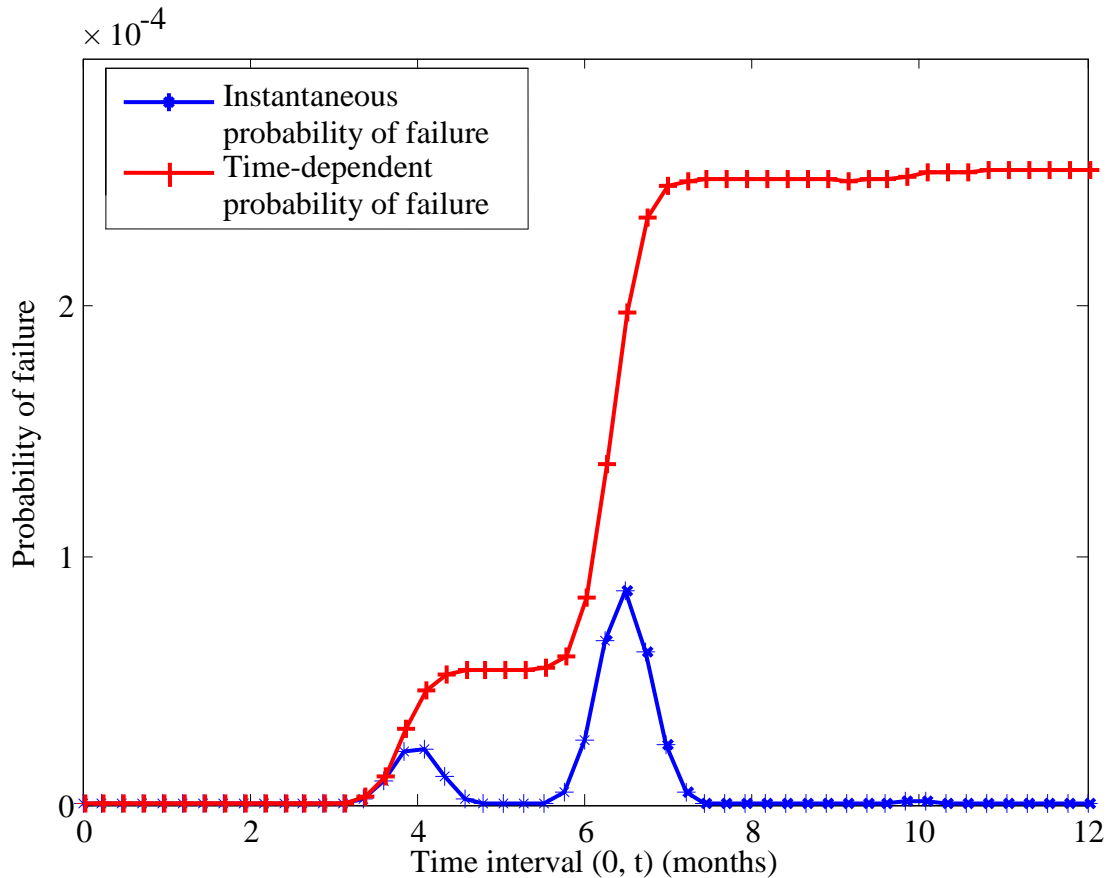
3

4

**Fig. 14** Probability of failure of the hydrokinetic turbine blades

1 4.3.2 Instantaneous probability of failure

2 We also calculated the instantaneous probability of failure. Fig.15 shows such instantaneous  
3 probabilities and time-dependent probabilities of failure over different time periods in a one-year  
4 time period.



5

6 **Fig. 15** Instantaneous and time-dependent probabilities of failure

7 It is seen that the time-dependent probability of failure is much larger than its instantaneous  
8 counterparts after the third month. The instantaneous probability of failure does not increase with  
9 time while it fluctuates over time. There are several peaks in the curve of the instantaneous  
10 probability of failure. The reason is the seasonal characteristics of the Missouri River flow  
11 velocity. At these peak points, the river velocities are large. Besides, it can be found that an

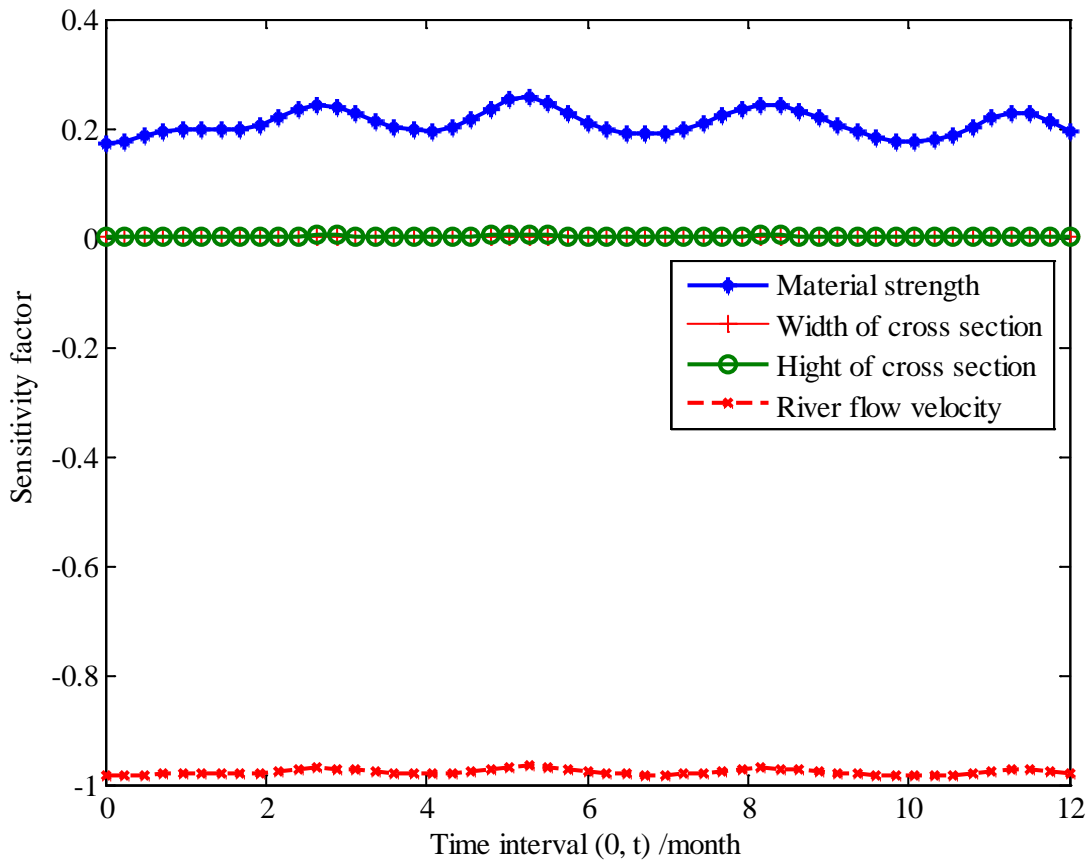


1 increasing slope of the instantaneous probability curve will results in an increase in the time-  
2 dependent probability of failure.

3

#### 4 4.3.3 Sensitivity analysis

5 As described in Sec. 3.4, the sensitivity factors show the relative importance of each random  
6 variable to the probability of failure. Fig. 16 provides the sensitivity factors of the four random  
7 variables when there is no cut-out river flow velocity for the turbine.



8

9

**Fig. 16** Sensitivity of random variables (without cut-out river velocity)

1 The results indicate that the river velocity and the material strength make the highest  
2 contributions to the probability of failure and that the dimension variables of the cross section at  
3 the root of the turbine blade make negligible contributions. Besides, the importance of random  
4 variables fluctuates with the time. The sensitivity factor of the material strength is positive, and  
5 this means that the probability of failure will decrease if the strength increases. On the contrary,  
6 the sensitivity factor of the river velocity is negative, and this indicates that the increase in the  
7 river velocity will result in the increase in the probability of failure. The river flow velocity is the  
8 most important contributor to the probability of failure of the hydrokinetic turbine blades. During  
9 the design stage, therefore, we should focus on the reduction of its effect on the reliability of the  
10 hydrokinetic turbine blades.

11

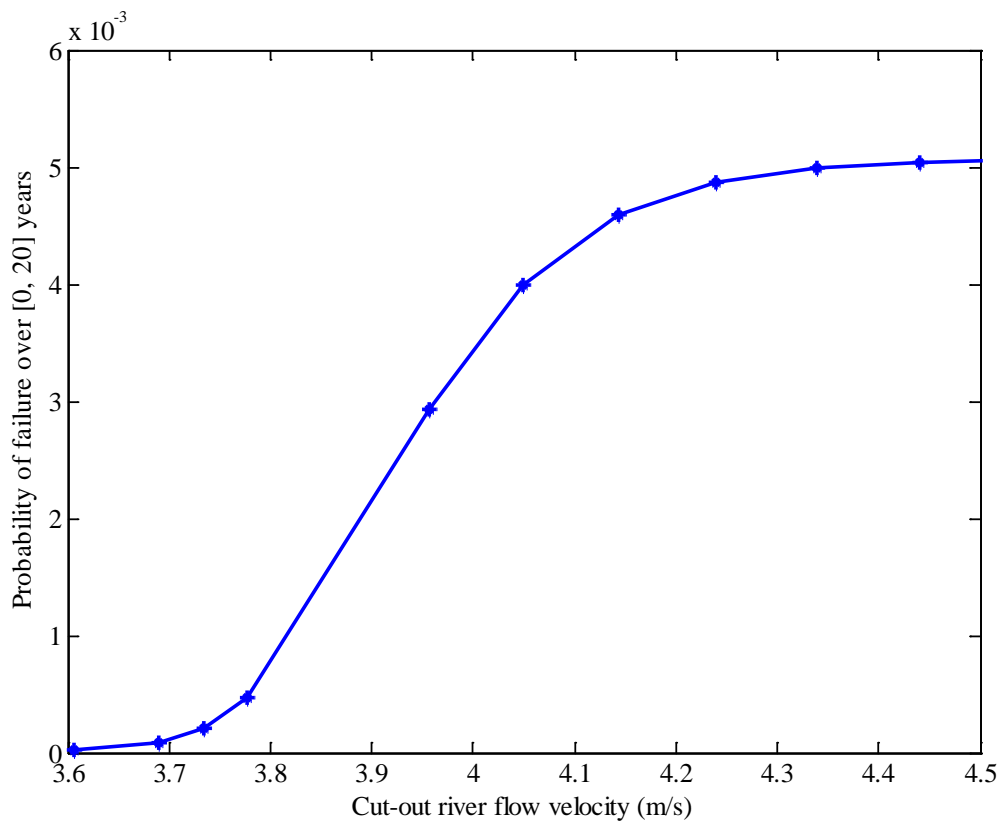
#### 12 *4.3.4 Influence of cut-out river flow velocity*

##### 13 (a) Effect on the probability of failure

14 To study the effect of the cut-out river flow velocity, we performed reliability analysis with  
15 different levels of cut-out river flow velocities. Fig. 17 provides the results over a 20-year time  
16 life. By comparing the results without a cut-out river velocity, we see that a proper cut-out river  
17 velocity can decrease the risk of failure significantly. For example, the probability of failure over  
18 a 20-year operation with a cut-out velocity of 3.7 m/s is about  $8.36 \times 10^{-5}$  while its counterpart  
19 without a cut-out velocity is  $5.1 \times 10^{-3}$ . This indicates that the upper tail of the river velocity  
20 makes a great contribution to the probability of failure.

21 The selection of a proper cut-out velocity is therefore important. From Fig. 17, we see that  
22 when the cut-out velocity is high over the range from 4.15 m/s to 4.5 m/s, the change in the

1 probability of failure will be slight with a reduced cut-out river velocity. When the cut-out  
2 velocity is between 3.7 m/s and 4.15 m/s, a reduced cut-out velocity can affect the probability of  
3 failure dramatically. Moreover, to determine the optimum cut-out river velocity, we should also  
4 consider the influence of the cut-out river velocity on the power output. If the cut-out river  
5 velocity is set to be very low, the reliability of the turbine blade will be high while the power  
6 output will be sacrificed. On the other hand, if the cut-out river velocity is very high, the  
7 reliability of the turbine may not be satisfied. This implies that the reliability analysis method  
8 developed in this paper can be integrated with the power output model and energy cost model of  
9 the hydrokinetic turbine system to identify the optimum cut-out river velocity for the  
10 hydrokinetic turbine system.

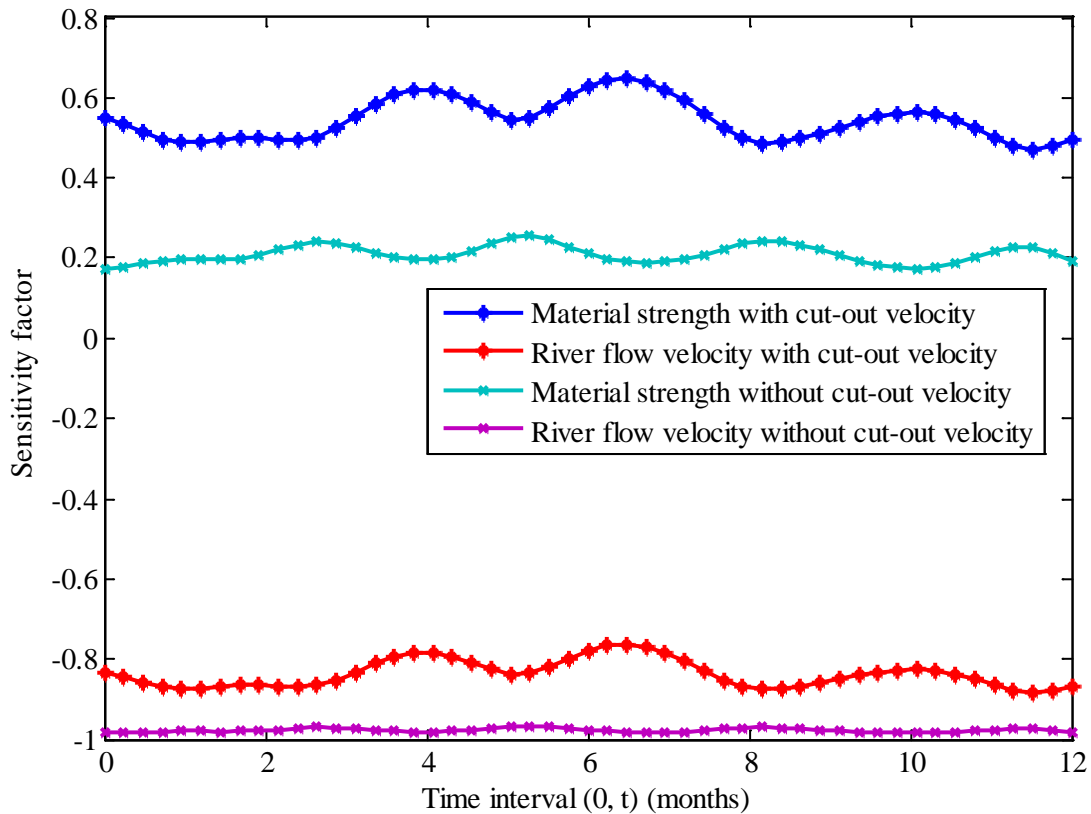


11

12 **Fig. 17** Time-dependent probability of failure of hydrokinetic turbine blades

1 (b) Effect on the sensitivity of random variables

2 To examine how the cut-out river velocity affects the sensitivity, we plot the sensitivity curves  
3 for the important variables with and without cut-out river velocity as shown in Fig. 18. These  
4 variables include the river flow velocity and material strength. A cut-out river velocity of 3.7 m/s  
5 was used for the analysis in Fig. 18.



6

7 **Fig. 18** Sensitivity of important random variables with and without cut-out river velocity

8 As shown in the figure, with the cut-out river velocity, the sensitivity factor of the river flow  
9 velocity decreases while that of the material strength increases. This indicates that by  
10 implementing a cut-out river velocity, we can reduce the sensitivity of the probability of failure  
11 with respect to the river velocity.

## 1 **5. Conclusions**

2 Reliability is an important factor to be considered during the hydrokinetic turbine design. The  
3 turbine blade reliability plays a critical role in the overall reliability of the hydrokinetic turbine  
4 system. In this work, we developed a time-dependent reliability analysis model for the  
5 hydrokinetic turbine blades. The blade element momentum theory was used to establish the  
6 limit-state function. The results show that the model can effectively evaluate the reliability of the  
7 hydrokinetic turbine blade over a certain time period.

8 We analyzed both of the time-dependent reliability over a time period and instantaneous  
9 reliability at an instant of time. The results showed that the time-dependent probability of failure  
10 is much larger than the instantaneous ones. Sensitivity analysis revealed that the river flow  
11 velocity and material strength make the highest contributions to the probability of failure of the  
12 hydrokinetic turbine blade and that the sensitivity of the probability of failure with respect to the  
13 river flow velocity is the highest.

14 The analysis also showed that a cut-out velocity affects the reliability of the hydrokinetic  
15 turbine in the following two aspects: First, an appropriately selected cut-out river velocity can  
16 decrease the probability of failure of the blade significantly. Second, with a cut-out river velocity,  
17 the contribution of the river flow velocity to the probability of failure decreases.

18 The pitch angle and tip speed ratio are assumed to be constant in this paper. But these  
19 parameters could be random. The cut-out velocity may also fluctuate in the real operation of the  
20 hydrokinetic turbine. These uncertainties will be considered in our future research. Even if the  
21 time-dependent reliability analysis model developed in this paper is based on the simplified  
22 models (the blade element momentum theory), it can be applied to more advanced models, such  
23 as the CFD and FEM simulations. In this work, we did not consider the spatial variation of the

1 river flow velocity. We only treated it as a stochastic process. Our future work will account for  
2 the spatial variation of the flow velocity, and we will then model the velocity as a time-  
3 dependent random field.

4

## 5 **Acknowledgment**

6 The authors gratefully acknowledge the support from the Office of Naval Research through  
7 contract ONR N000141010923 (Program Manager - Dr. Michele Anderson) and the Intelligent  
8 Systems Center at the Missouri University of Science and Technology.

9

## 10 **References**

- 11 [1] M.J. Khan, G. Bhuyan, M.T. Iqbal, J.E. Quaioco, Hydrokinetic energy conversion systems and  
12 assessment of horizontal and vertical axis turbines for river and tidal applications: A technology status  
13 review, *Applied Energy*, 86 (2009) 1823-1835.
- 14 [2] M. Veronica. B, Laura A, Schaefer, Computational fluid dynamics for hydrokinetic turbines,  
15 *Proceedings of the ASME 2009 International Mechanical Engineering Congress & Exposition,*  
16 *IMECE2009*, November 13-19, Lake Buena Vista, Florida, USA, 399-409.
- 17 [3] A.S. Bahaj, Generating electricity from the oceans, *Renewable and Sustainable Energy Reviews*, 15  
18 (2011) 3399-3416.
- 19 [4] P. Duvoy, H. Toniolo, HYDROKAL: A module for in-stream hydrokinetic resource assessment,  
20 *Computers and Geosciences*, (2011).
- 21 [5] V.J. Ginter, J.K. Pieper, Robust gain scheduled control of a hydrokinetic turbine, *IEEE Transactions*  
22 *on Control Systems Technology*, 19 (2011) 805-817.
- 23 [6] B.K. Kirke, Tests on ducted and bare helical and straight blade Darrieus hydrokinetic turbines,  
24 *Renewable Energy*, 36 (2011) 3013-3022.
- 25 [7] E. Lalander, M. Leijon, In-stream energy converters in a river - Effects on upstream hydropower  
26 station, *Renewable Energy*, 36 (2011) 399-404.

- 1 [8] H. Arabian-Hoseynabadi, H. Oraee, P.J. Tavner, Failure Modes and Effects Analysis (FMEA) for  
2 wind turbines, *International Journal of Electrical Power and Energy Systems*, 32 (2010) 817-824.
- 3 [9] S. Kahrobaee, S. Asgarpoor, Risk-based failure mode and effect analysis for wind turbines (RB-  
4 FMEA), in: *NAPS 2011 - 43rd North American Power Symposium*, art. no. 6025116 2011.
- 5 [10] P. Agarwal, *Structural reliability of offshore wind turbines*. The University of Texas at Austin, 2008.
- 6 [11] K. Saranyasootorn, L. Manuel, A comparison of wind turbine design loads in different  
7 environments using inverse reliability techniques, *Journal of Solar Energy Engineering, Transactions of*  
8 *the ASME*, 126 (2004) 1060-1068.
- 9 [12] K. Saranyasootorn, L. Manuel, Efficient models for wind turbine extreme loads using inverse  
10 reliability, *Journal of Wind Engineering and Industrial Aerodynamics*, 92 (2004) 789-804.
- 11 [13] K.O. Ronold, G.C. Larsen, Reliability-based design of wind-turbine rotor blades against failure in  
12 ultimate loading, *Engineering Structures*, 22 (2000) 565-574.
- 13 [14] P.H.A.J.M. W. Wang, Van Gelder and J.K. Vrijling, Long-memory in streamflow processes of the  
14 yellow river, *IWA International Conference on Water Economics, Statistics, and Finance Rethymno,*  
15 *Greece, 8-10 July, (2005) 481-490.*
- 16 [15] K. Breitung, Asymptotic approximations for the outcrossing rates of stationary vector processes,  
17 *Stochast Process Appl.*, 13 (1988) 195–207.
- 18 [16] G. Schall, M.H. Faber, R. Rackwitz, Ergodicity assumption for sea states in the reliability estimation  
19 of offshore structures, *Journal of Offshore Mechanics and Arctic Engineering*, 113 (1991) 241-246.
- 20 [17] F.M.H. Schall G, Rackwitz R., The ergodicity assumption for sea states in the reliability estimation  
21 of offshore structures. , *J Offshore Mech Arctic Engng.*, 113 (1991) 241–246.
- 22 [18] S. Engelund, R. Rackwitz, C. Lange, Approximations of first-passage times for differentiable  
23 processes based on higher-order threshold crossings, *Probabilistic Engineering Mechanics*, 10 (1995) 53-  
24 60.
- 25 [19] R. Rackwitz, Computational techniques in stationary and non-stationary load combination - A review  
26 and some extensions, *Journal of Structural Engineering (Madras)*, 25 (1998) 1-20.
- 27 [20] B. Sudret, Analytical derivation of the outcrossing rate in time-variant reliability problems, *Structure*  
28 *and Infrastructure Engineering*, 4 (2008) 353-362.
- 29 [21] J. Zhang, X. Du, Time-dependent reliability analysis for function generator mechanisms, *Journal of*  
30 *Mechanical Design, Transactions of the ASME*, 133 (2011).
- 31 [22] N. Vincent, Danny, Sale, Flow Characteristics of River Resources for Hydrokinetic Energy  
32 Conversion, in: *Proc. Conf. Proc., HydroVision International, July 27-30, 2010, Charlotte, NC, 2010.*
- 33 [23] L.B. Leopold, Downstream change of velocity in river, *American Journal of Science*, 251 (1953)  
34 606-624.

- 1 [24] V.K. Arora, G.J. Boer, A variable velocity flow routing algorithm for GCMs, *Journal of Geophysical*  
2 *Research D: Atmospheres*, 104 (1999) 30965-30979.
- 3 [25] K. Schulze, M. Hunger, P. Döll, Simulating river flow velocity on global scale, *Advances in*  
4 *Geosciences*, 5 (2005) 133-136.
- 5 [26] P.M. Allen, J.G. Arnold, B.W. Byars, Downstream channel geometry for use in planning-level  
6 models, *Water Resources Bulletin*, 30 (1994) 663-671.
- 7 [27] L.a.M. Leopold, T, The hydraulic geometry of stream channels and some physiographic implications,  
8 *Professional Paper 252*, United States Geological Survey, (1953).
- 9 [28] J.J. Beersma, T.A. Buishand, Joint probability of precipitation and discharge deficits in the  
10 Netherlands, *Water Resources Research*, 40 (2004) 1-11.
- 11 [29] L. Březková, M. Starý, P. Doležal, The real-time stochastic flow forecast, *Soil and Water Research*, 5  
12 (2010) 49-57.
- 13 [30] H.T. Mitosek, On stochastic properties of daily river flow processes, *Journal of Hydrology*, 228  
14 (2000) 188-205.
- 15 [31] I. Portoghese, E. Bruno, N. Guyennon, V. Iacobellis, Stochastic bias-correction of daily rainfall  
16 scenarios for hydrological applications, *Natural Hazards and Earth System Science*, 11 (2011) 2497-2509.
- 17 [32] P. Carl, H. Behrendt, Regularity-based functional streamflow disaggregation: 1. Comprehensive  
18 foundation, *Water Resources Research*, 44 (2008).
- 19 [33] P. Claps, A. Giordano, F. Laio, Advances in shot noise modeling of daily streamflows, *Advances in*  
20 *Water Resources*, 28 (2005) 992-1000.
- 21 [34] R. Krzysztofowicz, K.S. Kelly, Hydrologic uncertainty processor for probabilistic river stage  
22 forecasting, *Water Resources Research*, 36 (2000) 3265-3277.
- 23 [35] M. Muste, K. Yu, T. Pratt, D. Abraham, Practical aspects of ADCP data use for quantification of  
24 mean river flow characteristics; Part II: Fixed-vessel measurements, *Flow Measurement and*  
25 *Instrumentation*, 15 (2004) 17-28.
- 26 [36] M. Muste, K. Yu, M. Spasojevic, Practical aspects of ADCP data use for quantification of mean river  
27 flow characteristics; Part I: Moving-vessel measurements, *Flow Measurement and Instrumentation*, 15  
28 (2004) 1-16.
- 29 [37] M.Y. Otache, M. Bakir, Z. Li, Analysis of stochastic characteristics of the Benue River flow process,  
30 *Chinese Journal of Oceanology and Limnology*, 26 (2008) 142-151.
- 31 [38] O.L.H. Martin, *Aerodynamics of wind turbines*, Second edition, Earthscan, Sterling, VA., 2008.
- 32 [39] J.F. Manwell, J. G. McGowan *Wind Energy Explained: Theory, Design and Application*. New York,  
33 John Wiley and Sons., 2002.



- 1 [40] F. Akgül, D.M. Frangopol, Lifetime performance analysis of existing steel girder bridge  
2 superstructures, *Journal of Structural Engineering*, 130 (2004) 1875-1888.
- 3 [41] A.A. Czarnecki, A.S. Nowak, Time-variant reliability profiles for steel girder bridges, *Structural*  
4 *Safety*, 30 (2008) 49-64.
- 5 [42] P.H. Madsen, and Krenk, S., An integral equation method for the first passage problem in random  
6 vibration, *Journal of Applied Mechanics* 51 (1984) 674-679.
- 7 [43] S.O. Rice, Mathematical Analysis of Random Noise, *Bell System Technical Journal*, , 23 (1944)  
8 282-332.
- 9 [44] S.O. Rice, Mathematical analysis of random noise, *Bell Syst.Tech. J.*, 24 (1945) 146-156.
- 10 [45] S.K. Choi, R.V. Grandhi, R.A. Canfield, *Reliability-based structural design*, Springer, 2007.
- 11 [46] Z. Kala, Sensitivity analysis of the stability problems of thin-walled structures, *Journal of*  
12 *Constructional Steel Research*, 61 (2005) 415-422.
- 13 [47] A.C.H. David J. Laino, National Renewable Energy Laboratory Report, Report Number: NREL/TP-  
14 442-7817 Appendix B, in, 2002.
- 15 [48] R.D. Database, Gaylord Nelson Institute for Environmental Studies, University of Wisconsin-  
16 Madison, [http://www.sage.wisc.edu/riverdata/scripts/station\\_table.php?qual=32&filenum=1457](http://www.sage.wisc.edu/riverdata/scripts/station_table.php?qual=32&filenum=1457), in.
- 17 [49] D.L. Allaix, V.I. Carbone, Numerical discretization of stationary random processes, *Probabilistic*  
18 *Engineering Mechanics*, 25 (2010) 332-347.
- 19 [50] C.-C. Li, A. Der Kiureghian, Optimal discretization of random fields, *Journal of Engineering*  
20 *Mechanics*, 119 (1993) 1136-1154.